



# Silver Nanoflowers as an Interfacial Liquid-State Surface Enhanced Raman Spectroscopy (SERS) Sensor for Water Pollution

Zinah Salahuddin Shakir<sup>1,2\*</sup>, Ayad Abdul Razzak Dhaigham<sup>3</sup>, and Sameer Khudhur Yaseen<sup>4</sup>

<sup>1</sup> Institute of Laser for Postgraduate Studies, University of Baghdad, Baghdad, Iraq.

<sup>2</sup> Department of Applied Sciences, University of Technology, Baghdad, Iraq.

<sup>3</sup> Directorate of Materials Research, Ministry of Science & Technology, Baghdad, Iraq.

<sup>4</sup> Department of Physics, College of Science for Women, University of Baghdad, Baghdad, Iraq.

\*Email address of the Corresponding Author: [zena.salahaldeen1101a@ilps.uobaghdad.edu.iq](mailto:zena.salahaldeen1101a@ilps.uobaghdad.edu.iq)

**Article history:** Received 18 July 2023; Revised 2 Aug 2023; Accepted 14 Aug 2023; Published online 15 Dec 2023

**Abstract:** Water pollution has created a critical threat to the environment. A lot of research has been done recently to use surface-enhanced Raman spectroscopy (SERS) to detect multiple pollutants in water. This study aims to use Ag colloid nanoflowers as liquid SERS enhancer. Tri sodium phosphate ( $\text{Na}_3\text{PO}_4$ ) was investigated as a pollutant using liquid SERS based on colloidal Ag nanoflowers. The chemical method was used to synthesize nanoflowers from silver ions. Atomic Force Microscope (AFM), Scanning Electron Microscope (SEM), and X-ray diffractometer (XRD) were employed to characterize the silver nanoflowers. This nanoflowers SERS action in detecting  $\text{Na}_3\text{PO}_4$  was reported and analyzed concerning both shape and size using a 532 nm laser. We observed that the nanoflower's structure produced strong SERS signals. The increase in the SERS signal is related to the deposition of  $\text{Na}_3\text{PO}_4$  molecules in the aggregated silver nanostructure in the solution. The concentration of  $\text{Na}_3\text{PO}_4$  plays a main role in detection since the Raman signal becomes stronger as the concentration increases. The highest phosphate analytical enhancement factor obtained for SERS in colloidal nanoflowers was  $1.7 \times 10^3$  at  $0.7 \times 10^{-6}$  M which was the lowest concentration.

**Keywords:** AgNFs, Hotspot, Raman spectroscopy, Tri Sodium phosphate, Surface Plasmon resonance.

## 1. Introduction

Water pollution, one of the world's challenges, results from fast industrialization and poses a severe environmental danger. Organic and inorganic contaminants, like organic dyes, heavy metals, pesticides, sulfides, and so on, harm the aquatic system [1-3]. One of these pollutants that are dangerous to human health is fertilizers tri-sodium phosphate, which we will address in this research, as it can cause permanent



damage to human kidneys, leading to death [4]. Raman spectroscopy is a method that employs the vibrational spectrum to detect chemical interactions in a molecule and also being sensitive to surrounding changes [5]. As a consequence, Raman spectroscopy is a valuable tool for chemical and physical study. The Raman spectrum offers information particular to a substance, allowing for molecular identification [6]. Furthermore, Raman spectroscopy necessitates a simple preparation of the sample [7]. Raman signals are typically weak, but they can be significantly increased by adsorbing molecules on a roughened surface of metal or metal nanoparticles. This technique is known as surface-enhanced Raman spectroscopy (SERS) [8]. SERS is considered an effective optical sensing process to detect various analytes. The SERS impact has been linked to an improvement in the effectiveness of Raman scattering for molecules that are present on or very close to the surface of specific metal nanostructures, particularly free-electron metals like gold, silver, and copper. As a result, chemically or physically adsorbed molecules on these metal nanostructures experience a considerable Raman signal increase. SERS is capable of detecting even a single molecule and achieving very large enhancement factors (more than  $10^{10}$ ) with appropriate metal nanostructures and measurement settings [2,9]. The most frequently accepted explanations for SERS are the electromagnetic mechanism (EM) and the chemical mechanism (CM) [10,11]. EM has been reported to be more significant than CM [12]. EM is primarily based on surface plasmon in a metal nanostructure [13, 14]. In the EM process, electromagnetic waves interact with plasmonic metal nanostructures which leads to amplifying the Raman signal [15,16]. SERS has evolved into a valuable instrument for the quantitative study of hazardous compounds, even at low levels in food and the environment. SERS substrates are metal nanostructures that increase the Raman spectral signature of molecules deposited on them. SERS substrates can be of two different natures: colloidal nanoparticles in solution or nanostructures deposited on a surface [17]. It is commonly assumed that the significant Raman signal increase in SERS results from electromagnetic motivation at 'hot spots' on the SERS substrate [9,18,19]. These 'hot spots' are often nanogaps between neighboring metal nanostructures or narrow areas surrounding metal nanostructure tips [18,19]. Because of the number of 'hot spots,' experimental research and theoretical calculations have revealed that complex silver nanostructures including dendritic, flower-like, and star-like nanostructures can give an extremely high increase in the electromagnetic field [20-21].

This study will focus on the flower-like silver nanostructure as a liquid SERS substrate to demonstrate the detection of tri-sodium phosphate as a pollutant in water. Several research teams have created flower-like silver nanostructures known as silver nanoflowers-AgNFs to be used as SERS substrates [2].

## 2. Experimental work

### 2.1. Materials and methods

Tri-sodium phosphate ( $\text{Na}_3\text{PO}_4$ ), and silver nitrate ( $\text{AgNO}_3$ ) were purchased from CDH, India, and ascorbic acid (AA,  $\text{C}_6\text{H}_8\text{O}_6$ ) tri-sodium citrate di-hydrate ( $\text{TSC C}_6\text{H}_5\text{Na}_3\text{O}_7 \cdot 2\text{H}_2\text{O}$ ), polyvinylpyrrolidone (PVP) were purchased from SABIC, KSA, De-ionized (DI) water

### 2.2. Synthesis of silver nanoflower

First, an ice water bath arrangement was prepared by placing a 50 mL beaker holding 20 mL of distilled water in a 250 mL beaker having ice cubes. This configuration was exposed to 400 rpm magnetic stirring. After 10 minutes, a 0.5 M aqueous solution of  $\text{AgNO}_3$  (2 mL) was added to the water. For another 10 minutes, the solution was treated with 0.3 M PVP aqueous solution (2 mL). The solution was then treated with 0.25 M tri-sodium citrate di-hydrate (0.2 mL) at 10-minute intervals. After 10 minutes, 0.5 M of AA (2 mL) was poured into the previously stated solution while stirring constantly [2]. A dark grey solution was obtained. A scanning electron microscope (SEM) AxiaChemiSEM by Thermo Scientific, the Netherlands, and an atomic force microscope (AFM) Model TT-2 AFM workshop, USA, were used to examine the surface morphologies and nanoparticle size distributions of the prepared Ag nanoflower. An



X-ray diffractometer (XRD) was applied to measure the crystallographic information of the Ag nanoflower in the range from 10 to 80. An ultraviolet-visible (UV-Vis) spectrophotometer was utilized to investigate the absorption spectrum of  $\text{Na}_3\text{PO}_4$ .

### 2.3. Preparation of Samples for SERS Spectra

Four samples of  $\text{Na}_3\text{PO}_4$  were prepared at concentrations ( $0.7 \times 10^{-3}$ ,  $0.7 \times 10^{-4}$ ,  $0.7 \times 10^{-5}$ , and  $0.7 \times 10^{-6}$ ) M in the Ag nanoflower colloidal. In order to make a comparison, we prepared a sample with a concentration of  $0.7 \times 10^{-3}$  M of  $\text{Na}_3\text{PO}_4$  in distilled water only. This bare sample will allow us to better understand the effects of the pollutant in question. SERS spectra samples were measured in a glass vial with the laser beam focused within. Raman scattering measurements were taken by using a Raman microscope (532 nm Preconfigured Raman Spectrometer System) by (Stellar Net, Inc. Florida, USA). Samples were stimulated by a 532 nm laser line generated by a laser with a power of 70 mW at the sample and an integration time of 9 ms. In all cases, the spectral resolution was adjusted to  $2 \text{ cm}^{-1}$ . SERS spectra were registered using a total acquisition time of 10s for each SERS spectrum and a single scan. All Raman measurements were taken in the spectral region ( $200 - 2000 \text{ cm}^{-1}$ ).

## 4. Results and Discussion

According to the SEM images in Fig.1, the size of silver nanoflower was approximately 400 nm. The nanoparticles were aggregated and formed hot spots which were thought to be the source of the substantial rise in signal strength required for single-molecule detection [22, 23].

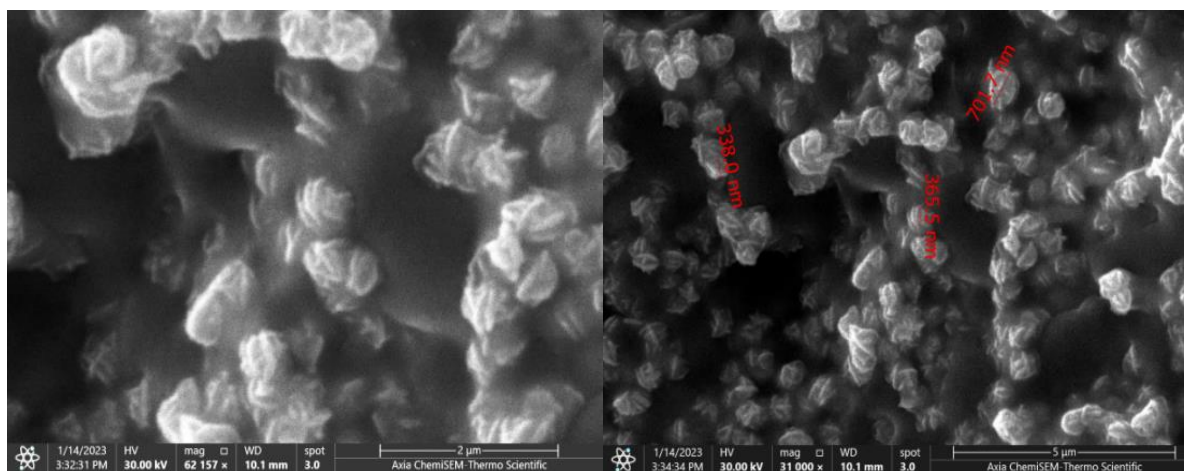


**Fig.1:** Scanning Electron microscope images for silver nanoflower.

According to the results obtained from the AFM, the average silver nanoparticle size was 13.61 nm; see Fig.2. The image shows that the nanosilver cluster formation in the topographic distribution is uniformly distributed. The test also revealed that the density of the silver nanoflower colloidal solution was 434 million particles/ $\text{mm}^2$ . The X-ray diffraction pattern of the AgNF structure exhibited unique diffraction peaks at ( $38.341^\circ$ ,  $64.656^\circ$ , and  $77.625^\circ$ ), which are similar to pure silver crystal planes (111), (220), and (331); see Fig.3. These strong peaks in the planes suggest that the AgNFs are extremely crystalline. There were no further impurity peaks found, indicating that the samples were extremely pure. The crystalline size of Ag-NF was calculated from the Debye – Scherer equation and the average value of it was 43.6 nm [24].

$$L = k \lambda / \beta \cos \theta_B \quad (1)$$

Where  $L$ ,  $k$ ,  $\lambda$ ,  $\beta$ , and  $\theta_B$  are the crystalline size, the shape factor value which equals 0.9, the wavelength of the X-ray in nm, full width at half maximum (FWHM) in radians, and the diffraction angle in radians respectively. It is clear from Fig.4 that the absorption spectrum of  $\text{Na}_3\text{PO}_4$  is approximately 200 nm which makes the 532 nm laser used in the Raman measurement suitable hence it is not very close to the absorbance area that produces fluorescence.

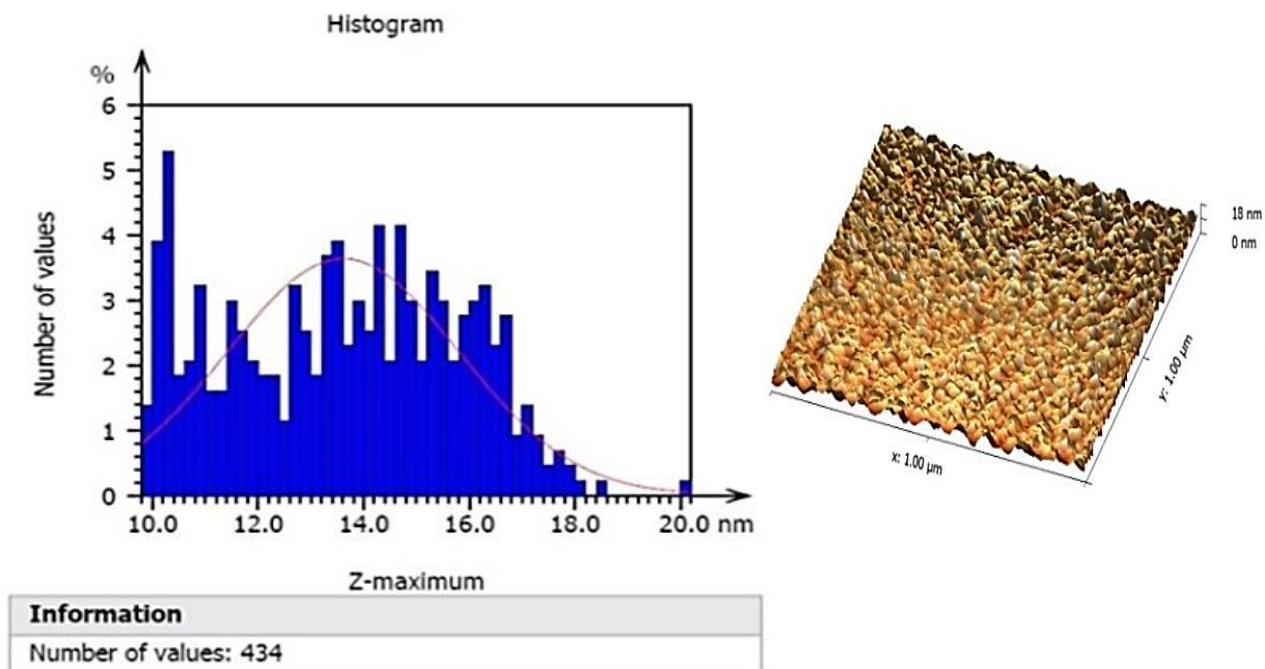


**Fig.2:** AFM analysis: Granularity cumulation distribution histogram and AFM- 3 dimensions image of silver nanoflower.

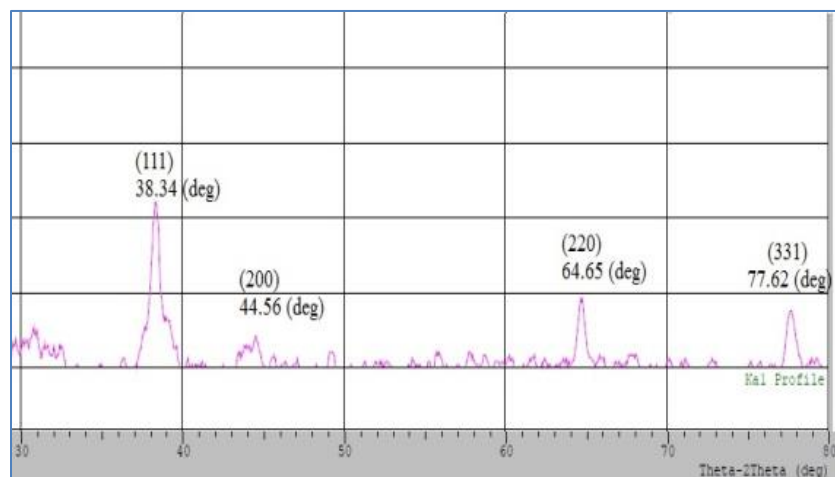


**Fig. 3:** Typical XRD pattern of AgNFs that have been synthesized.

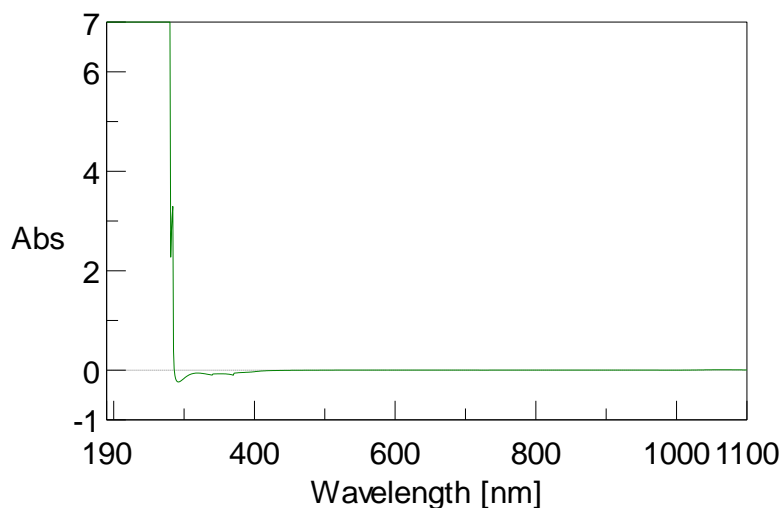


**Fig.4:** The absorption spectrum of Na<sub>3</sub>PO<sub>4</sub>.

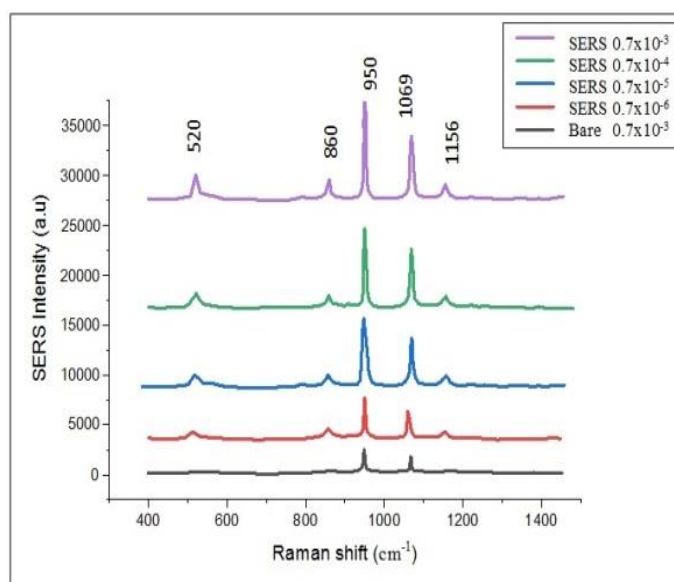


**Fig.5:** SERS intensity at the main peak (950 cm<sup>-1</sup>) of Raman spectrum for Na<sub>3</sub>PO<sub>4</sub> against the concentrations of Na<sub>3</sub>PO<sub>4</sub> in Ag nanoflowers colloids.

The samples containing AgNFs showed greater Raman intensities at all Raman peaks than the bare ones; see Fig.5. It has been linked to the massive hotspots generated by the sharp edges and nanogaps of AgNFs structure when subjected to laser light [2,25]. A significant local electromagnetic field is generated around the surface of the nanostructure which can be up to 100 times stronger than the incident one [26], resulting in a significant amplification of the Raman signal. This strong local electromagnetic field resulted from the excitement of localized surface plasmon (LSP), which correlates with collective oscillations of the cloud of electrons within nanostructures, or electromagnetic interaction between nanostructures. [27,28]. Based on previous research, it has been found that the greatest increase in hot spot enhancement occurs when the distance between nanoparticles is reduced and the particle diameter is smaller, especially when the surface curvature increases [29]. The electromagnetic coupling in the space between the nanoparticles is caused by

the nanoflowers aggregated in the solution. Due to the adjacency effect, the enhancement with the aggregated nanoparticles is more intense than for individual ones owing to forming electromagnetic "hot spot" in the nanoparticle gap, which produce a strong SERS signal from the molecules around it [17].

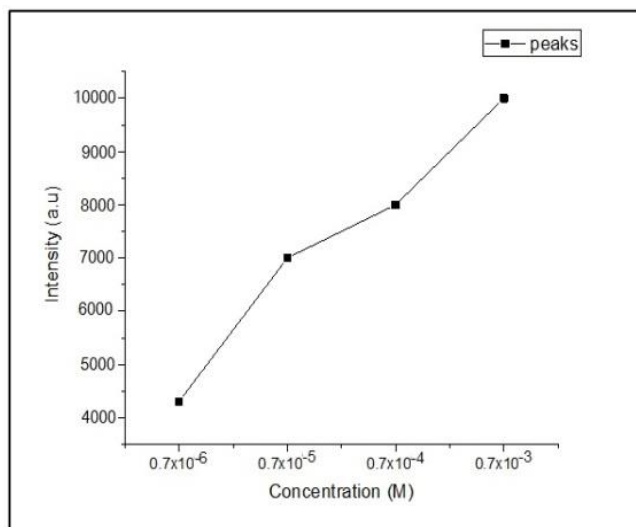


**Fig.6:** SERS intensity at the main peak ( $950 \text{ cm}^{-1}$ ) of Raman spectrum for  $\text{Na}_3\text{PO}_4$  against the concentrations of  $\text{Na}_3\text{PO}_4$  in Ag nanoflowers colloids.

The relationship between the concentrations of  $\text{Na}_3\text{PO}_4$  and SERS intensity has shown in Fig.6. It is obvious that when  $\text{Na}_3\text{PO}_4$  concentration increases, the SERS intensity increases too; this is attributed to the increase of the molecules of  $\text{Na}_3\text{PO}_4$  attracted to AgNFs, Thus the Raman signal will be strengthened so the enhance Raman scattering strengthen which agree with articles [8, 30].

The analytical enhancement factor (AEF) was utilized to assess the actual SERS enhancement produced by EM and CM. AEF takes an analytical method for signal enhancement, combining signal strength with analyte concentration (C). This measure is useful when estimating the amount of analyte molecules present is difficult, especially for analytes that have no specific affinity for the plasmonic surfaces. AEF influences the vibration mode of a specific analyte in a normal Raman signal in the SERS technique, and it is directly proportional to the strength of the local electromagnetic field, referred to as a hot spot [31, 8].

$$AEF = \frac{I_{\text{SERS}} \times C_{\text{NRS}}}{C_{\text{SERS}} \times I_{\text{NRS}}} \quad (2)$$

Where;  $I_{\text{NRS}}$  and  $I_{\text{SERS}}$  refer to the counterpart intensities of normal Raman and SERS, respectively,  $C_{\text{NRS}}$  and  $C_{\text{SERS}}$  are the concentrations of the analyte in the normal Raman and SERS liquid substrates, respectively.

Based on our analysis, there appears to be a nonlinear increase of AEF at the highest peak ( $950 \text{ cm}^{-1}$ ) as the concentration of  $\text{Na}_3\text{PO}_4$  decreases. This means that SERS is more efficient with lower concentrations. Overall, this information can help us better understand the effects of  $\text{Na}_3\text{PO}_4$  on the samples we are analyzing; see Fig.7. Very low molecule concentrations improve the probability of specific molecule localization, which leads to better detection and hence raises the AEF by enhancing the SERS signal. At  $0.7 \times 10^{-6} \text{ M}$ , the maximum phosphate AEF found for SERS in colloidal nanoflowers was  $1.7 \times 10^3$ . The variation in (AEF) was mostly related to the variation in overlaps between SPR bands as a function of edge size and degree and the laser source. For ultrasensitive detection of phosphate molecules, the electromagnetic process of aggregated AgNF creates multiple hotspots from plentiful nanogaps on nanoflowers [29].

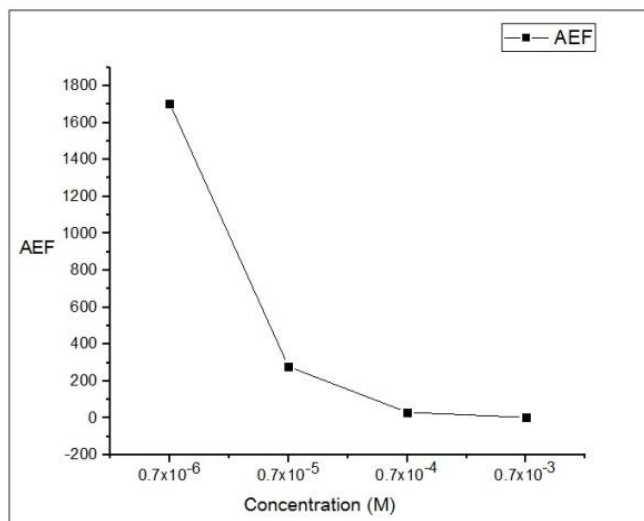


**Fig.7:** AEF at the main peak of SERS Raman intensity ( $950 \text{ cm}^{-1}$ ) against the concentration of  $\text{Na}_3\text{PO}_4$  in the Ag nanoflowers colloid.

## 5. Conclusions

Tri sodium phosphate was examined as a pollutant utilizing liquid SERS based on colloidal silver nanoflowers. The structure of nanoflowers with sharp edges and corners produced strong SERS signals. The aggregated nanoflowers in the colloidal have generated hot spots. When  $\text{Na}_3\text{PO}_4$  molecules are absorbed in solution and engage hot spots, the electromagnetic field increases, so the Raman signals are enhanced. The hot spot regions, which exist as minimal distances between nanoparticles, have an effect on the intense electromagnetic fields; SERS signals are greater within these microscopic hot spots. The AEF is directly proportional to the strength of the local electromagnetic field (a hot spot). The AEF influences the vibration mode of a specific analyte in a normal Raman signal in the SERS technique. As the  $\text{Na}_3\text{PO}_4$  concentration increased, so did the Raman peaks. At  $0.7 \times 10^{-6} \text{ M}$  (the lowest concentration), the highest phosphate AEF for SERS in colloidal nanoflowers was  $1.7 \times 10^3$  which means SERS is more efficient with lower concentrations.

## References

- [1] J. Wang, C. Qiu, X. Mu, H. Pang, X. Chen, D. Liu, "Ultrasensitive SERS detection of rhodamine 6G and p-nitrophenol based on electrochemically roughened nano-Au film", *Talanta*, **210**, 120631 (2020).
- [2] Nazar Riswana Barveen, Tzyy-Jiann Wang, Yu-Hsu Chang, "In-situ deposition of silver nanoparticles on silver nanoflowers for ultrasensitive and simultaneous SERS detection of organic pollutants". *Microchemical Journal*, **159**, 105520 (2020).
- [3] Manh Cuong Nguyen, Truc Quynh Ngan Luong, Thi Thu Vu, Cao Tuan Anh, Tran Cao Daoab, "Synthesis of wool roll-like silver nanoflowers in an ethanol/water mixture and their application to detect traces of the fungicide carbendazim by SERS technique". *RSC Adv.*, **12**, 11583-11590 (2022).
- [4] Wimalawansa SA, Wimalawansa SJ. Impact of changing agricultural practices on human health: Chronic kidney disease of multi-factorial origin in Sri Lanka. *Wudpecker J Agric Res.*, **3**(5), 110-24 (2014).
- [5] Durickovic, I. Using Raman spectroscopy for characterization of aqueous media and quantification o/f species in aqueous solution. In *Applications of Molecular Spectroscopy to Current Research in the Chemical and Biological Sciences*; Stauffer, M., Ed.; Intech: Rijeka, Croatia, 2016.
- [6] Leonardo M. Moreira, Landulfo Silveira Jr., Fábio V. Santos, Juliana P. Lyon, Rick Rocha, Renato A. Zângaro, Antonio Balbin Villaverde, Marcos T. T. Pacheco, "Raman spectroscopy: A powerful technique for biochemical analysis and diagnosis", *Journal of Spectroscopy*, **22**, 19 (2008).

- [7] Cyrankiewicz, M.; Wybranowski, T.; Kruszewski, S. "Study of SERS efficiency of metallic colloidal systems". In *Journal of Physics: Conference Series, Proceedings of the XIII International Seminar on Physics and Chemistry of Solids*, Ustron, Poland, IOP Publishing: Bristol, UK, **79**, 01203(2007).
- [8] Hidayah AN, Triyono D, Herbani Y, Saleh R. "Liquid Surface-Enhanced Raman Spectroscopy (SERS) Sensor-Based Au-Ag Colloidal Nanoparticles for Easy and Rapid Detection of Deltamethrin Pesticide in Brewed Tea". *Crystals*, **12**(1), 24(2022).
- [9] L. T. Q. Ngan, D. T. Cao, C. T. Anh, and L. V. Vu, "Trace detection of herbicides by SERS technique, using SERS-active substrates fabricated from different silver nanostructures deposited on silicon". *Int. J. Nanotechnol.*, **12**, 358 (2015).
- [10] Zhang Y, Mi X, Tan X, Xiang R. "Recent Progress on Liquid Biopsy Analysis using Surface-Enhanced Raman Spectroscopy". *Theranostics*, **9**(2):491-525 (2019).
- [11] Fromm, D.P.; Sundaramurthy, A.; Kinkhabwala, A.; Schuck, P.J.; Kino, G.S.; Moerner, W.E. "Exploring the chemical enhancement for surface-enhanced Raman scattering with Au bowtie nanoantennas". *J. Chem. Phys.*, **124**, 61101(2006).
- [12] Davies, R.A.; Chong, N.S.; Ooi, B.G. "Chemical enhancement of the surface enhanced Raman scattering signals of anilines via their Ortho-substituents". *Opt. Photonics J.*, **3**, 13–23(2013).
- [13] Ding, S.Y.; You, E.M.; Tian, Z.Q.; Moskovits, M. "Electromagnetic theories of surface-enhanced Raman spectroscopy". *Chem. Soc. Rev.*, **46**, 4042–4076 (2017).
- [14] Wang, J.; Lin, W.; Cao, E.; Xu, X.; Liang, W.; Zhang, X. "Surface plasmon resonance sensors on Raman and fluorescence spectroscopy". *Sensors*, **17**, 2719 (2017).
- [15] Ling, Y.; Zhuo, Y.; Huang, L.; Mao, D. "Using Ag-embedded TiO<sub>2</sub> nanotubes array as recyclable SERS substrate". *Appl. Surf. Sci.*, **388**, 169–173 (2016).
- [16] Roguska, A.; Kudelski, A.; Pisarek, M.; Opara, M.; Janik-Czachor, M. "Surface-enhanced Raman scattering (SERS) activity of Ag, Au and Cu nanoclusters on TiO<sub>2</sub>-nanotubes/Ti substrate". *Appl. Surf. Sci.*, **257**, 8182–8189 (2011).
- [17] Raymond Gillibert, Jiao Qi Huang, Yang Zhang, Wei Ling Fu, Marc Lamy de la Chapelle. "Explosive detection by Surface Enhanced Raman Scattering". *TrAC Trends in Analytical Chemistry*. **105**, 166-172 (2018).
- [18] H. Tang, C. Zhu, G. Meng and N. Wu, J. "Review—Surface-Enhanced Raman Scattering Sensors for Food Safety and Environmental Monitoring". *Electrochem. Soc.*, **165**, B3098 (2018).
- [19] T. C. Dao, T. Q. N. Luong, T. A. Cao and N. M. Kieu. Fabrication of Silver Nanodendrites on Copper for Detecting Rhodamine 6G in Chili Powder Using Surface-enhanced Raman Spectroscopy. *Adv. Nat. Sci. Nanosci. Nanotechnol.*, **10**, 025012(2019).
- [20] H. B. Li, P. Liu, Y. Liang, J. Xiao and G. W. Yang. "Super-SERS-active and highly effective antimicrobial Ag nanodendrites". *Nanoscale.*, **4**, 5082(2012).
- [21] Y. Han, S. Liu, M. Han, J. Bao, and Z. Dai, "Fabrication of Hierarchical Nanostructure of Silver via a Surfactant-Free Mixed Solvents Route". *Cryst. Growth Des.*, **9**, 3941–3947(2009).
- [22] A. Garcia-Leis, J. V. Garcia-Ramos, and S. Sanchez-Cortes. "Silver Nanostars with High SERS Performance". *J. Phys. Chem. C*, **117**, 7791(2013).
- [23] C. S. Kumar. "Raman spectroscopy for nanomaterials characterization. Springer Science & Business Media", 2012.
- [24] Francisco M. L., Felipe M. M., Paulo H., Ana F., and Francisco N. "Nanostructured titanium dioxide average size from alternative analysis of Scherrer's Equation" *revista. Matéria*, **23**(1), (2018).
- [25] J. Tong, Z. Xu, Y. Bian, Y. Niu, Y. Zhang, Z. Wang. "Flexible and smart fibers decorated with Ag nanoflowers for highly active surface-enhanced Raman scattering detection. *J. Raman Spectrosc.*", **50**, 1468–1476(2019).
- [26] E. C. Le Ru, P. G. Etchegoin, "Quantifying SERS enhancements". *MRS Bull*, **38**, 631- 640 (2013).
- [27] N. Guillot, M. L. de la Chapelle, "The electromagnetic effect in surface enhanced Raman scattering: Enhancement optimization using precisely controlled nanostructures". *J. Quant. Spectrosc. Radiat. Transf.*, **113**, 2321–2333(2012).
- [28] M J. Grand, et al. "Role of localized surface plasmons in surface-enhanced Raman scattering of shape-controlled metallic particles in regular arrays". *Phys Rev B*, **72**, 033407(2005).
- [29] Robert C. Maher. "Raman Spectroscopy for Nanomaterials Characterization" *SERS Hot Spots.*, Chapter 10, 215–260. (2012).
- [30] McLellan JM, Siekkinen A, Chen J, Xia Y. "Comparison of the surface-enhanced Raman scattering on sharp and truncated silver Nanocubes". *Chemical Physics Letters*. **427**(1-3), 122-6(2006).
- [31] W. Plieth, H. Dietz, A. Anders, G. Sandmann, A. Meixner, M. Weber, H. Knepppe. "Electrochemical preparation of silver and gold nanoparticles: Characterization by confocal and surface enhanced Raman microscopy". *Surface Science*, **597**(1–3), 119-126 (2005).





## محلول الفضة الغروي النانوي الزهري الشكل كمستشعر مطياف رامان المحسن للسطح للكشف عن ملوثات المياه

زينة صلاح الدين شاكر\*<sup>1,2</sup> ، اياد عبد الرزاق ضيغم<sup>3</sup> ، سمير خضر ياسين<sup>4</sup>

<sup>1</sup>معهد الليزر للدراسات العليا، جامعة بغداد، بغداد، العراق.

<sup>2</sup>قسم العلوم التطبيقية، الجامعة التكنولوجية، بغداد، العراق.

<sup>3</sup>دائرة بحوث المواد، وزارة العلوم والتكنولوجيا بغداد، العراق

<sup>4</sup> قسم الفيزياء، كلية العلوم للبنات، جامعة بغداد، بغداد، العراق.

\*البريد الإلكتروني للباحث: [zena.salahaldeen1101a@ilps.uobaghdad.edu.iq](mailto:zena.salahaldeen1101a@ilps.uobaghdad.edu.iq)

**الخلاصة:** قد خلق تلوث المياه تهديداً خطيراً للبيئة ، وقد تم إجراء الكثير من الأبحاث مؤخراً لاستخدام مطيافية رامان المعززة على السطح (SERS) لاكتشاف الملوثات المتعددة في المياه. تهدف هذه الدراسة إلى استخدام الفضة النانوية الغروية الزهرية ككاشف محسن السطح لتقنية رامان. تم فحص ثلاثي فوسفات الصوديوم ( $\text{Na}_3\text{PO}_4$ ) باعتباره ملوثاً باستخدام SERS السائل بناءً على محلول الفضة الغرواني الزهري الشكل . تم استخدام الطريقة الكيميائية لتجميع الزهور النانوية من أيونات الفضة. تم استخدام مجهر القوة الذرية (AFM) ، والمجهر الماسح الإلكتروني (SEM) ، ومقياس حيود الأشعة السينية (XRD) لتوصيف الزهور النانوية الفضية. تم تقييم إجراء SERS هذا في الكشف عن الفوسفات وتحليله فيما يتعلق بكل من الشكل والحجم باستخدام ليزر 532 نانومتر. لاحظنا أن البنية الزهرية للفضة النانوية الغروية أنتجت إشارات SERS قوية. ترتبط الزيادة في إشارة SERS بترسيب جزيئات  $\text{Na}_3\text{PO}_4$  في البنية النانوية للفضة المتكتلة في المحلول. يلعب تركيز الفوسفات دوراً رئيسياً في الكشف حيث تصبح إشارة رامان أقوى مع زيادة التركيز. كان أعلى معامل للتحسين التحليلي للفوسفات الذي تم الحصول عليه لـ SERS في زهور النانو الغروية  $1.7 \times 10^3$  عند  $0.7 \times 10^{-6}$  مولار والذي كان أقل تركيز.

